THE JOURNAL OF BIOLOGICAL CHEMISTRY VOL. 281, NO. 23, pp. 16117–16127, June 9, 2006

Specification of SUMO1- and SUMO2-interacting Motifs*[S]

Received for publication, November 29, 2005, and in revised form, March 7, 2006 Published, JBC Papers in Press, March 8, 2006, DOI 10.1074/jbc.M512757200

Christina-Maria Hecker[‡1,2], **Matthias Rabiller**[§1], **Kaisa Haglund**[‡], **Peter Bayer**[§3], **and Ivan Dikic**[‡4]

From the [‡]*Institute for Biochemistry II, Goethe University Medical School, Theodor-Stern-Kai 7, 60590 Frankfurt, Germany and the* [§]*Universität Duisburg-Essen, Fachbereich Biologie und Geografie, Strukturelle und Medizinische Biochemie, Universitätsstrasse, 45117 Essen, Germany*

SUMO proteins are ubiquitin-related modifiers implicated in the regulation of gene transcription, cell cycle, DNA repair, and protein localization. The molecular mechanisms by which the sumoylation of target proteins regulates diverse cellular functions remain poorly understood. Here we report isolation and characterization of SUMO1- and SUMO2-binding motifs. Using yeast two-hybrid system, bioinformatics, and NMR spectroscopy we define a common SUMO-interacting motif (SIM) and map its binding surfaces on SUMO1 and SUMO2. This motif forms a β-strand that could bind in parallel or antiparallel orientation to the β_2-strand of SUMO due to the environment of the hydrophobic core. A negative charge imposed by a stretch of neighboring acidic amino acids and/or phosphorylated serine residues determines its specificity in binding to distinct SUMO paralogues and can modulate the spatial orientation of SUMO-SIM interactions.

SUMO proteins are small ubiquitin (Ub)[5]-related modifiers that become conjugated to cellular substrates and regulate diverse cellular processes including cell cycle progression, intracellular trafficking, transcription, and DNA repair (1–3). Like Ub, a SUMO protein is covalently attached to target proteins through an isopeptide bond by a mechanism similar to that of ubiquitination, which involves E1, E2, and E3 enzymes (4). In mammals, three SUMO paralogues are commonly expressed: SUMO1 shares about 45% identity to SUMO2 and SUMO3, while SUMO2 and SUMO3 are 96% identical to each other (2, 5).

The structures of all three SUMO paralogues resemble the globular and compact Ub-like fold (6, 7). The differences of SUMO1 and SUMO2 are mostly found in the second β-strand and the α-helix of both proteins (7). In cells, different SUMO paralogues appear to share common properties but also have some distinct functions. For example, the promyelocytic leukemia protein is conjugated to all three SUMO paralogs (8, 9), whereas RanGAP1 is preferentially modified with SUMO1 (10) and topoisomerase II with SUMO2/3 during mitosis (11). Furthermore, the distribution of the SUMO paralogues within cells seems to be different. SUMO1 is uniquely found within the nucleoli, the nuclear envelope, and cytoplasmic foci, whereas SUMO2/3 are accrued on chromosomes at an earlier point in the nuclear reformation process (12). Interestingly, there is a larger pool of free, non-conjugated SUMO2/3 than of SUMO1 (10).

In addition to targeting different substrate proteins, the functional properties of SUMO isoforms *in vivo* might also reflect their ability to mediate distinct protein-protein interactions. Indeed, recent studies have shown that SUMO paralogues can promote non-covalent binding to other proteins containing specific motifs that recognize SUMO paralogues. Minty and coworkers defined a Ser-Xaa-Ser motif surrounded by hydrophobic and acidic amino acids as a SUMO-interacting motif (SIM) (13). Biophysical studies of the SIM in PIAS revealed that the small hydrophobic region is an essential determinant of SUMO recognition (14). Moreover, the SUMO-binding motif was proposed as Lys-Xaa_{3-5}-[Val/Ile]-[Ile/Leu]$_2$-Xaa_3-[Asp/Glu/Gln/Asn]-[Asp/Glu]$_2$ in yeast proteins (15). Recent publications revealed that the hydrophobic core can bind both parallel and antiparallel to SUMO (16, 17). It is thought that sumoylated targets may control cell functions depending on their ability to interact with effectors containing SUMO-binding motifs. However, most of the SUMO interacting studies were done with the SUMO1 paralogue.

In this study we describe the identification and characterization of novel SUMO1- and SUMO2-binding partners containing a universal SIM. The molecular and structural details are presented explaining the basis for SIM binding to distinct SUMO paralogues. We show that the E3 ligase PIASxα is phosphorylated *in vivo* within the SIM and that phosphorylation influences its binding to SUMO1 but not to SUMO2. In the case of TTRAP, a protein that binds SUMO2 much stronger than SUMO1, and PIASxα we show that negative charged amino acids surrounding the hydrophobic core influence binding to SUMO1 but not to SUMO2.

EXPERIMENTAL PROCEDURES

Yeast Two-hybrid Screen—Sequences corresponding to SUMO1(ΔGG) and SUMO2(ΔGG) were subcloned in pYTH9 vector between SalI and BglII restriction site creating fusion proteins with Gal4-DNA-binding domain. Both vectors were introduced using lithium acetate/polyethylene glycol transfomation with herring testis carrier DNA into Y190 yeast strain cDNA libraries were then similarily introduced and transformed cells were grown on agar plates containing a synthetic dropout medium (BD Bioscience) without leucine, tryptophan, histidine, and with 25 mM 3-amino-1,2,4-triazole. Colonies that grew on the selection medium were transferred to a filter and assayed for β-galactosidase activity with substrate X-gal (5-bromo-4-chloro-3-indolyl-βD-galactopyranoside).

Plasmid DNA was extracted using a glass bead disruption method and were amplified by transformation and lysis of DH5α bacteria. Plasmids were then retransformed into yeast containing the bait to confirm binding and grown on the same agar plates as described above. After X-gal test plasmids were sequenced.

* This work was supported by grants from the Deutsche Forschungsgemeinschaft (DI 931/1-1) and Boehringer Ingelheim Fonds (to I. D.). The costs of publication of this article were defrayed in part by the payment of page charges. This article must therefore be hereby marked "*advertisement*" in accordance with 18 U.S.C. Section 1734 solely to indicate this fact.

[S] The on-line version of this article (available at http://www.jbc.org) contains supplemental Figs. 1–3.

[1] These authors contributed equally to this work.
[2] Fellow of the Hessian Ministry for Science and Arts.
[3] To whom correspondence may be addressed. E-mail: Peter.Bayer@uni-due.de.
[4] To whom correspondence may be addressed. E-mail: Ivan.Dikic@biochem2.de.

[5] The abbreviations used are: Ub, ubiquitin; SIM, SUMO-interacting motif; UIM, ubiquitin-interacting motif; X-gal, 5-bromo-4-chloro-3-indolyl-β-D-galactopyranoside; HA, hemagglutinin; GST, glutathione *S*-transferase; GFP, green fluorescent protein; EGFP, enhanced GFP; YFP, yellow fluorescent protein; HSQC, heteronuclear single quantum coherence; MALDI, matrix-assisted laser desorption ionization; SH, Src homology; UBD, Ub-binding domain.

To compare the strength of interaction between SUMO1 and SUMO2, 1.5 μg of each plasmid were retransformed in yeast containing SUMO1 and SUMO2 in parallel and grown on the agar plates described above. After 6 days three different colonies (if colonies grew at all) were replicated to another agar plate. After 3 days colonies were transferred to a filter to compare the growth of yeast containing SUMO1 and SUMO2 and the interacting partners.

Plasmids and Mutagenesis—HA-TTRAP-pcDNA3 plasmid was described previously (18). HA-TTRAP SUMO-binding mutants were generated with site-directed mutagenesis by PCR using QuikChange (Stratagene). HA-TTRAP SIM mutant was constructed using the primer pair 5′-TTACCCAACAACGCTGCGGATGTCTGGGAGTTTTTG-3′ and 5′-CAAAAACTCCCAGACATCCGCAGCGTTGTTGGGTAA-3′ introducing two alanines and primer pair 5′-CCCAACAACGCTGCGGCTGCCTGGGAGTTTTTGGGCAAA-3′ and 5′-TTTGCCCAAAAACTCCCAGGCAGCCGCAGCGTTGTTGGG-3′ to introduce two further alanines. GST-SUMO2 and YFP-UBC9 were kindly provided by Frauke Melchior and FLAG-PIAS1, GST-SUMO1, and FLAG-PIAS2 (PIASxα) by Jorma Palvimo. GST-TTRAP was generously provided by Danny Huylebroeck.

Acidic deletion mutants were constructed using site-directed mutagenesis. Sequences of the primers are available upon request. FLAG-PIAS3 was kindly provided by Helene Boeuf and FLAG-Sp100 and EGFP-Sp100 by Hans Will.

Cell Culture and Transfections, Cell Lysis, GST Pulldown, SDS-PAGE, and Western Blot—All these techniques were done as described before (19). The HA antibody was used from Santa Cruz Biotechnology, FLAG M2 antibody form Sigma and GFP/YFP antibody form BD Bioscience.

Protein Expression and Purification for NMR Studies—Full-length SUMO1 and SUMO2 were cloned as GST fusions into pET-41a vectors (Novagen), expressed in bacteria on either LB medium (for non-marked protein) or minimal medium with $^{15}NH_4Cl$ and [$^{13}C_6$]glucose for labeled protein. The recombinant protein was purified on a GSH resin (Amersham Biosciences) according to manufacturer's instruction and cleaved with thrombin, leaving the extension Gly-Ser in N-term of the full length SUMO; concentrators (Amicon) were used for tag removal and concentration. The protein was lyophilyzed and stored at −20 °C.

NMR Spectra Acquisition and Assignment—All measurements were made at 27 °C in 25 mM Phosphate buffer at pH 7. Triple resonance and two-dimensional experiments were performed on a Varian Inova 600 equipped with shielded *Z* gradients. Three-dimensional NMR spectra were processed using the standard Bruker software XWINNMR. Two-dimensional NMR spectra were processed using NMRpipe (42). Analysis and visual representation of two-dimensional spectra were performed using Sparky (T. D. Goddard and D. G. Kneller, University of California, San Francisco), and three-dimensional spectra were analyzed with the program Aurelia (Bruker). Assignment of SUMO2 was generated using the spectra HNCA, HNCACB, CBCA(CO)NH, HC(CO)NH, and C(CO)NH.

NMR Titration Experiments—For peptide titration experiments heteronuclear single quantum coherence (HSQC) spectra were performed on ^{15}N-labeled SUMO1 or SUMO2 (300 mM in 25 mM phosphate buffer, pH 7). Unlabeled peptides were chemically synthetized by Thermo Electron GmbH, dissolved to a concentration of 2.7 mM in 25 mM phosphate buffer, pH 7, and titrated to the protein to reach a final peptide:SUMO ratio of 1.36:1. No precipitation could be observed even at the highest peptide concentrations. K_D values were measured by two different methods, depending on the exchange regime. For amino acids in fast exchange regime, at each titration step, the distance of each peak from its original position was measured using the normalization proposed before (20). The obtained curves were fitted to a Hill 4-parameter model using the software SigmaPlot.

Bioinformatical Analysis—All sequence data base searches were performed with a non-redundant data set constructed from current releases of Swiss-Prot, TrEMBL, and GenPept (21, 22). Generalized profile construction (23) and searches were run locally using the pftools package, version 2.1. Generalized profiles were constructed using the BLOSUM45 substitution matrix (24) and default penalties of 2.1 for gap opening and 0.2 for gap extension. The statistical significance of profile matches was derived from the analysis of the score distribution of a randomized data base (25).

Tryptic Digestion of PIAS and Detection of the Resulting Fragments by MALDI Spectrometry—HEK 293T cells were transfected with FLAG-PIAS and lysed, and the FLAG-PIAS expression was checked with Western blot analysis as described before. Immunoprecipitation of FLAG-PIAS was done with M2-agarose from Sigma according to manual instruction. Immunoprecipitated PIAS was loaded on SDS-PAGE gel and stained with Coomassie. The band containing PIAS was cut out of the gel and transferred into a microtube. As a negative control, a same sized bit of the gel cut from a region containing no protein and further handled as the probe. Except the digestion itself, all further steps were performed at room temperature under agitation (1000 rpm). The band was destained overnight using 0.5 ml of acetic acid/methanol/water 1:2:7 (v:v:v). It was washed for 4 h with water, dried with a SpeedVac, washed with (50% acetonitrile, 50% 0.2 M NH_4HCO_3 in water, pH 8.9), and dried with a SpeedVac again. The band was soaked with 15 μl of 0.2 M NH_4HCO_3 in water, pH 8.9, containing 33 $\mu g \cdot ml^{-1}$ trypsin proteomic grade (Sigma). The gel was reduced into little bits using the heat-rounded tip of a pasteur pipette and incubated at 37 °C for 24 h. The bits were washed with water for 2 h, dried with a SpeedVac, and covered with 50 μl of formic acid/water/isopropanol 1:3:2 (v:v:v) saturated with α-cyano-4-hydroxycinnamic acid. After overnight incubation, tubes were opened to allow crytallisation of the α-cyano-4-hydroxycinnamic acid together with the extracted peptides. The obtained solution was pipetted onto the MALDI plate avoiding to pipette gel bits. Measurements were made in reflector-positive mode, low mass gate set at 500 Da, and monitoring the 1–3-kDa range.

RESULTS

Identification of SUMO1- and SUMO2-interacting Partners—To identify proteins that non-covalently bind to SUMO1 and SUMO2, we fused SUMO1 and SUMO2 mutants lacking two C-terminal glycine residues to the Gal4-DNA-binding domain of the YTH9 bait vector and performed large scale yeast two-hybrid screens using human thymus, spleen, and kidney libraries. After retransformation and X-gal tests we sequenced 102 SUMO1-interacting and 77 SUMO2-interacting partners. In this collection, we subsequently identified about 20 different candidate SUMO-interacting proteins, including SUMO-conjugating enzyme (UBC9), thymine DNA glycosylase (TDG), TOPORS, four members of the PIAS family, and RanBP2, which have been previously shown to interact with SUMO1 or SUMO2 (13, 14, 26). Altogether, we identified 10 new candidate SUMO-interacting proteins for which no data about sumoylation or SUMO interaction are available (Fig. 1*A*). Among these proteins there were several zinc finger-containing proteins including ZCCHC7, ZCCHC12, ZNF237, ZNF198, and ZHX1 involved in different processes like DNA repair or transcriptional repression (27, 28). Moreover, Senataxin, a newly identified helicase mutated in patients suffering from ataxia-ocular apraxia 2, was found to interact with SUMO proteins in our screens (29). So far, two helicases,

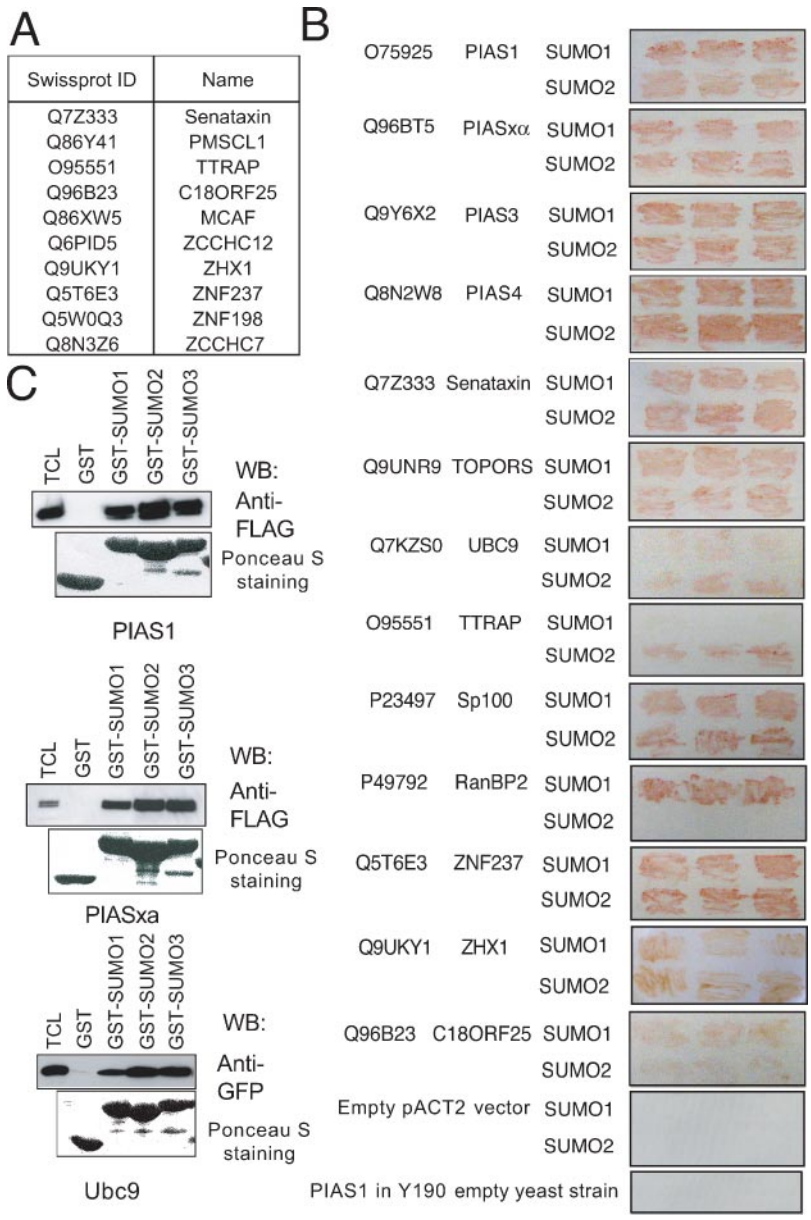

FIGURE 1. **Yeast two-hybrid screen.** *A*, table of the newly identified SUMO-interacting proteins with their Swiss-Prot ID and name. *B*, growth of yeast containing SUMO1 or SUMO2; each prey plasmid was retransformed into yeast containing either SUMO1 or SUMO2 as bait in parallel. Yeast was grown on agar plates containing the appropriate drop out medium. After 4 days three different colonies were replated on another agar plate and incubated at 30 degrees. After 3 days yeast was transferred to a filter and growth was compared. *First column*, Swiss-Prot ID; *second column*, name of the prey; *third column*, three replicates of yeast clones, retransformed with prey and either SUMO1 or SUMO2. *C*, confirmation of yeast two-hybrid results with GST pulldown assays for PIAS1, PIAS2 (isoform xα), and UBC9 using HEK 293T cells transfected with PIAS1, PIAS2, or UBC9 and GST-SUMO1/2/3. GST alone was used as negative control. Western blots were performed with antibodies against the FLAG epitope and YFP. Levels of GST fusion proteins were determined by Ponceau S staining. *TCL*, total cell lysate.

the BLM helicase and Werner's helicase, are known to be sumoylated and play important roles in causing hereditary diseases (30, 31). The findings of new SUMO-interacting partners underline the important function of SUMO signals during transcription, DNA repair, and chromatin remodeling (32).

We next investigated whether these SUMO-interacting proteins bind preferentially to SUMO1 or SUMO2 in yeast cells. We retransformed all clones found to bind to SUMO1 in yeast expressing SUMO2 and in yeast expressing SUMO1 in parallel. The same was done for all the clones found to bind to SUMO2. As a control we transformed empty prey vector in yeast containing SUMO1 and SUMO2, while PIAS1, which was shown to interact strongly with SUMO1 and SUMO2, was transformed into the empty yeast strain. To compare the binding affinity to SUMO1 and SUMO2 we re-plated three different colonies of each retransformation on another agar plate with appropriate drop out medium. After 2 days yeast was transferred on a filter paper to compare the growth. Most of the retransformed SUMO-interacting partners bound to SUMO1 and SUMO2 with the same strength (Fig. 1*B*), whereas RanBP2 preferentially bound to SUMO1, an interaction that was already shown to be important for its function (33), and TTRAP (TRAF and TNF receptor-associated protein), strongly bound to SUMO2 and poorly to SUMO1 (Fig. 1*B*). Nothing grew on the control plates. To compare binding affinities of SUMO1 and SUMO2 with SUMO3, we did *in vitro* pulldown assays for PIAS1, PIASxα, and UBC9 (Fig. 1*C*). As expected, SUMO3 bound with a similar affinity to these proteins as SUMO1 and SUMO2 did.

Characterization of SUMO-interacting Motif in TTRAP—TTRAP was originally found as a protein interacting with members of the tumor necrosis factor receptor (TNF-R) superfamily as well as several TRAFs (18). Since TTRAP bound more potently to SUMO2 than SUMO1 in yeast (Fig. 1*B*), we analyzed the interactions between SUMO1 and SUMO2 with TTRAP in more details. When cell lysates expressing HA-TTRAP were incubated with beads coupled to GST, GST-SUMO1, GST-SUMO2, or GST-SUMO3, TTRAP bound more potently to SUMO2 and SUMO3 than to SUMO1 (Fig. 2, *A* and *B*). TTRAP did not contain one of the published SUMO-binding domains. However, we could find the sequence I-V-D-V at positions 280–284, which is the inversion of the proposed V/I-*X*-V/I-V/I

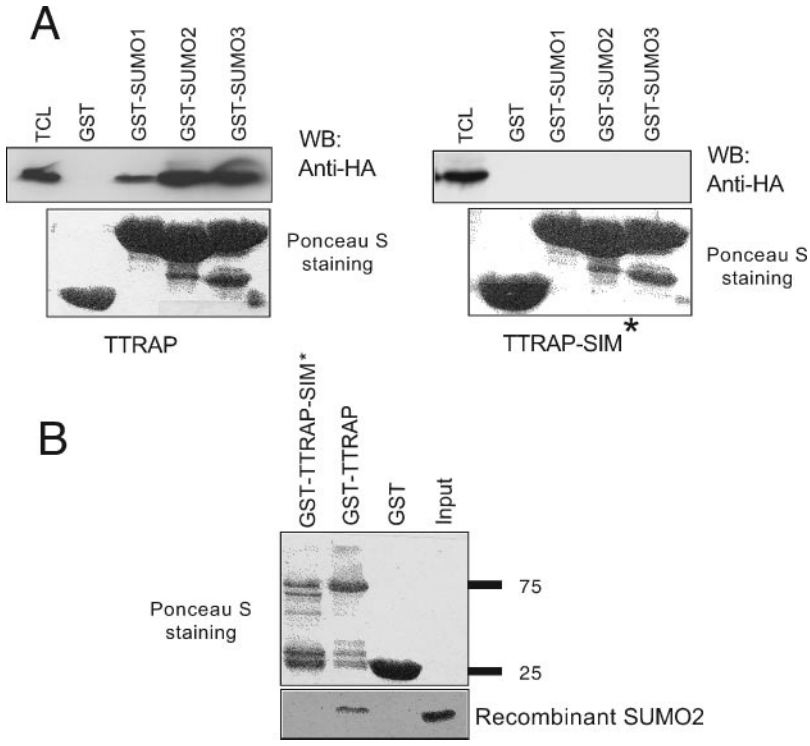

FIGURE 2. **New SUMO-interacting motif in TTRAP.** *A*, HEK 293T cells were transiently transfected with wild type HA-TTRAP. Cell lysates were subsequently incubated with GST alone or GST-SUMO1/2/3. HA-TTRAP wild type binds strongly to SUMO2 and SUMO3 and weaker to SUMO1. Repetition of the GST pulldown assay with cells expressing a mutant of the potential SUMO-interacting motif (TTRAP-SIM*) revealed that binding to all SUMO isoforms can be abolished. Western blots were performed with anti-HA antibodies. Levels of GST fusion proteins were determined by Ponceau staining. *TCL*, total cell lysate; *aa*, amino acids. *B*, GST pulldowns of purified SUMO2 with GST, GST-TTRAP, and GST-TTRAP-SIM* detected by Ponceau S staining to analyze direct interaction.

SUMO-interacting motif (14). Recently, it was shown that this hydrophobic part could bind both parallel and antiparallel to SUMO so that these four amino acids could be a SUMO-binding domain as well (17). We mutated all four amino acids to alanine (HA-TTRAP-SIM*) and completely abolished binding to all SUMO isoforms (Fig. 2*B*). Since these binding assays were performed in yeast and mammalian cells, they raised a concern whether additional cellular proteins might contribute to indirect binding between SUMO and TTRAP. To verify their interaction *in vitro* system, full-length TTRAP and TTRAP-SIM* were expressed and purified as a GST fusion protein in bacteria and challenged with recombinant SUMO2. As shown in Fig. 2*C*, SUMO2 bound to GST-TTRAP but not to GST alone or GST-TTRAP-SIM*. This result confirmed that the SIM of TTRAP directly interacts with SUMO2 and that this signature motif is essential for SUMO binding to full size TTRAP.

Definition of a Universal SIM—Three different amino acid signature motifs have been proposed to mediate binding to SUMO (Fig. 3*A*). To identify minimal SIMs in newly cloned SUMO-interacting proteins, the sequences of the clones were subjected to bioinformatical analyses. All of the three proposed sequence motifs implicated in binding to SUMO are represented in both known and new SUMO-interacting partners pooled in our screens (Fig. 3*B*). Interestingly, several SUMO-interacting partners contain two SUMO-binding domains. Some SUMO-interacting partners, including TTRAP, MCAF, and ZCCHC12, do not contain the complete characteristics of any of the published domains but rather represent the inversion of motif 2 (Fig. 3*B*).

An alignment of all SUMO-interacting motifs revealed that they all harbored a hydrophobic core sequence consisting of stretches of three or four hydrophobic Ile, Leu, or Val residues plus one acidic/polar residue at position 2 or 3. The sequences surrounding this core-binding domain are predicted to be disordered and have a net negative charge due to a stretch of acidic amino acid residues (Fig. 3*C*). The stretch of acidic amino acids can be either at the C- or at the N-terminal site of the hydrophobic core. Furthermore, a spacer containing a conserved threonine can separate the hydrophobic part from the acidic one. Interestingly, the majority of SIMs contains one or more serines or threonines, being potential phosphorylation sites *in vivo*.

Biophysical Parameters Underlying Binding of SIMs to Different SUMO Paralogues—We used NMR spectroscopy to gain detailed insights into the binding of different SIM motifs to SUMO1 or SUMO2. In typical NMR titrations, binding of a ligand to a protein influences the environment of the atoms of the protein, especially in the binding interface between the protein and the ligand. Such perturbations are easily observable as modification of the frequency and intensity of resonances in HSQC spectra during a titration experiment. We used the already published assignment of SUMO1 (34) and measured a set of three-dimensional spectra to assign the resonances of all atoms in the backbone and side chains of SUMO2 (supplemental Fig. 1).

To characterize the binding interface on SUMO paralogues and different SIMs we chose to study the SIMs of PIASxα, which interact with equal strength with SUMO1 and SUMO2 (Fig. 1, *B* and *C*) and contain a stretch of acidic amino acids and several putative serine phosphorylation sites. We also analyzed the SIM of TTRAP, which interacts predominantly with SUMO2 *in vivo* and *in vitro* experiments and lacks the acidic tract. Thus, three different PIASxα peptides and one TTRAP peptide were synthesized to investigate the binding characteristics of SUMO1 and SUMO2 to these peptides (Fig. 4*A* and supplemental Fig. 2).

Most of the amino acids in slow exchange in the titrations of SUMO1 and SUMO2 with $SIM_{PIASx\alpha}$ are found in the β_2-strand and α-helix of those proteins (Fig. 4, *B* and *C*). The K_D associated with the amino acids in slow exchange is estimated to be 3 μM for SUMO1 and 2 μM for SUMO2, which is in good agreement with the results derived from isothermal titration calorimetry measurements (14).

The binding surface of the other peptides (SIM_{TTRAP}, $SIM_{pPIASx\alpha}$, $SIM_{PIASx\alpha\ short}$) was found to be on the same position on SUMO1 and SUMO2 showing that this surface represents a general binding surface

A

Motif 1	h-h-X-[S]-[X]-[S/T]-a-a-a	Minty et al
Motif 2	[V/I]-X-[V/I]-[V/I]	Song et al
Motif 3	K-X_{3-5}-[I/V]-[I/L]-[I/L]-X_3-[D/E/Q/N]-[D\E]-[D/E]	Hannich et al

B

Swissprot ID	Name	Strength of interaction with SUMO1	Strength of interaction with SUMO2	SUMO binding motif
O75925	PIAS1	++++	++++	motif 1
Q96BT5	PIAS2	++++	++++	motif 1
Q9Y6X2	PIAS3	++++	++++	motif 1
Q8N2W8	PIAS4	++++	++++	motif 1
P49792	RanBP2	++++		motif 2
Q7Z333	Senataxin	++++	++++	motif 1
P23497	SP 100C	+++	++++	motif 1
Q86Y41	PMSCL1	+	+	motif 2
Q96B23	C18ORF25	++	++	motif 2
O95551	TTRAP	+	+++	inverted motif 2
Q86XW5	MCAF	+	+	inverted motif 2
Q6PID5	ZCCHC12	++	++	inverted motif 2
Q9UNR9	TOPORS	+++	+++	motif 1
Q9UKY1	ZHX1	+++	+++	motif 1
Q5T6E3	ZNF237	++++	++++	motif 3
Q5W0Q3	ZNF198	+	+	motif 3
Q8N3Z6	ZCCHC7	++	++	motif 1

C

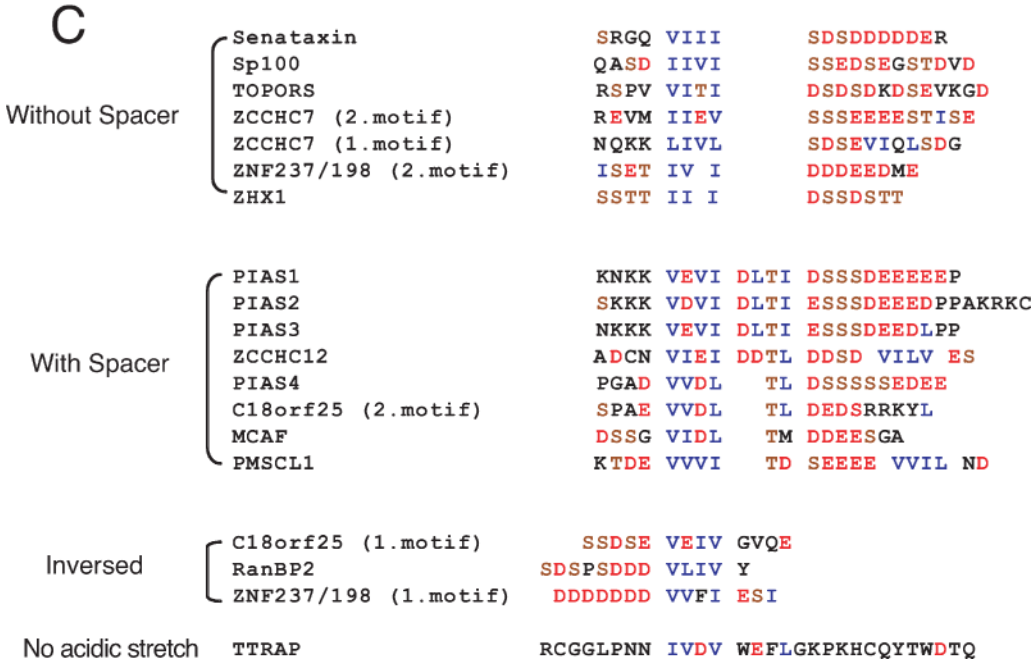

FIGURE 3. **Definition of universal SIM.** *A*, three published SUMO-binding motifs: "*h*" represents a hydrophobic amino acid and "*a*" an acidic one. *B*, summary of the clones found in all screens, their Swiss-Prot IDs, and their names and strength of interaction to SUMO1 and SUMO2 in the screen are shown. Some SUMO-interacting partners like TTRAP, MCAF, and ZCCHC12 do not contain one of the published domains. *C*, alignment of SUMO-interacting motifs of the yeast clones. All motifs contain a hydrophobic core (*blue*), acidic amino acids (*red*), and/or potential phosphorylation sites (*brown*).

for the SIM on SUMO (Fig. 4*D*). Since this surface is partly constituted by a side of the β-sheet of SUMO, and the hydrophobic core of the SIM has a sequence typical of a β-strand, we propose that the hydrophobic core of the SIM binds to the β_2-strand of SUMO by forming an intermolecular β-sheet.

Serine Phosphorylation in the SIM of PIASxα Regulates Its Binding to SUMO1—According to the K_D values $SIM_{PIASx\alpha}$ binds with similar affinity to SUMO1 and SUMO2. However, the curves of these two titrations have different shapes: Whereas the curves obtained in the titration of SUMO2 with $SIM_{PIASx\alpha}$ have the expected shape for a simple 1:1 protein to peptide binding, the curves obtained in the titration of SUMO1 with this peptide have an unexpected sigmoidal shape (Fig. 5*A*). Such curves are also observed in the titration of SUMO1 with $SIM_{PIASx\alpha\ short}$. The titration curves of SUMO1 and SUMO2 with $SIM_{pPIASx\alpha}$ have the classical shape, showing that the phosphorylation of the SIM is sufficient to change from one to the other binding

A

SIM_{PIASxa} KVDVIDLTIESSSDEEEDPPAKR

$SIM_{pPIASxa}$ KVDVIDLTIE(P)SSSDEEEDPPAKR

$SIM_{PIASxa\ short}$ VDVIDLTIES

SIM_{TTRAP} DTNLRDREVTRCGGLPNNIVDVW

B

SUMO1			SUMO2			
PIAS	pPIAS	PIAS-short	PIAS	pPIAS	PIAS-short	TTRAP
F36	**F36**	F36	**Q30**	**Q30**	**Q30**	Q30
V38	**V38**	V38	**F31**	**F31**	**F31**	
K39	**K39**	K39	**I33**	**I33**	**I33**	I33
M40	**M40**		K34	**K34**	**K34**	K34
T42	**T42**		T37	T37	T37	
H43	H43	H43	L39	L39	L39	
K45	**K45**	K45	**L42**	**L42**	**L42**	L42
S50	**S50**		**A45**	A45	A45	A45
Y51	**Y51**		**Y46**	**Y46**	Y46	
3 μM	**3 μM**		**2 μM**	**2 μM**	**2 μM**	

C

```
                1         11         21         31         41         51
                |         |          |          |          |          |
P63165_SUMO1    MSDQEAKPSTEDLGDKKEG-EYIKLKVIGQDSSEIHFKVKMTTHLKKLKESYCQRQGVPM 59
P55854_SUMO2    MSEEKPKE-----GVKTEN-DHINLKVAGQDGSVVQFKIKRHTPLSKLMKAYCERQGLSM 54
P61956_SUMO3    MADEKPKE-----GVKTENNDHINLKVAGQDGSVVQFKIKRHTPLSKLMKAYCERQGLSM 55
                *:::::.*       * *.*. ::*:*** ***.* ::**:*  * *.** ::**:***:.*

                61         71         81         91         101
                |          |          |          |          |
P63165_SUMO1    NSLRFLFEGQRIADNHTPKELGMEEEDVIEVYQEQTGGHSTV------- 101
P55854_SUMO2    RQIRFRFDGQPINETDTPAQLEMEDEDTIDVFQQQTGGVPESSLAGHSF 103
P61956_SUMO3    RQIRFRFDGQPINETDTPAQLEMEDEDTIDVFQQQTGGVY--------- 95
                ..:** *:** * :..** :* **:**.*:*:*:****
```

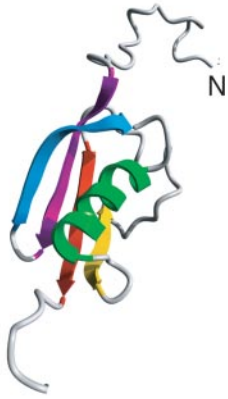

D

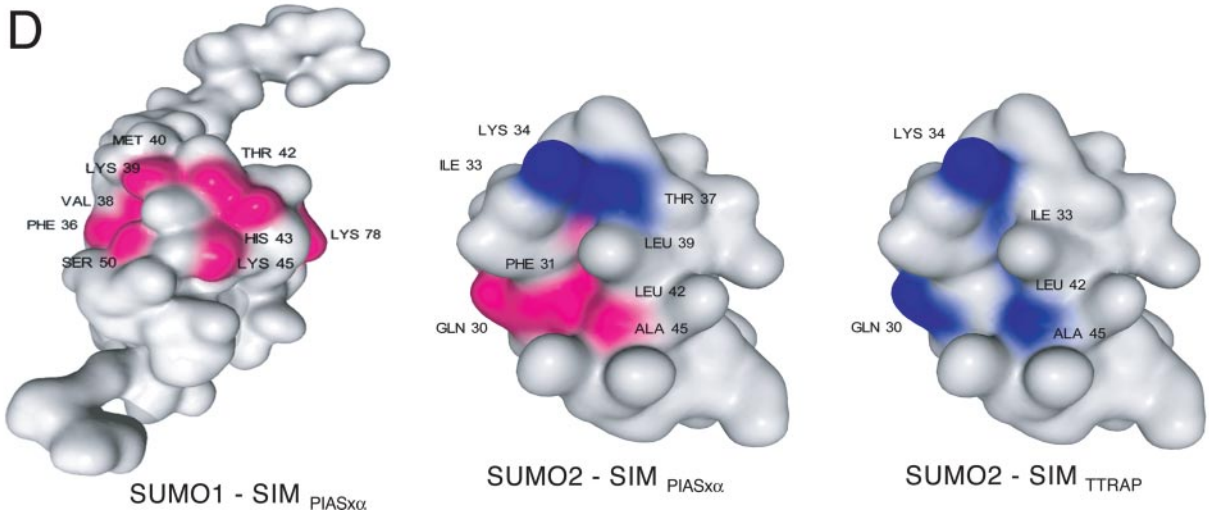

FIGURE 4. **Binding surface analysis.** *A*, alignment of peptides used for SUMO titrations. Negatively charged amino acids are in *red*, and positively charged amino acids are in *blue*. Phosphorylation is represented by a *circled P*. *B*, table with amino acids of SUMO1 and SUMO2 involved in binding to PIASxα and TTRAP peptides. Amino acids in slow exchange are indicated in *bold* and amino acids in intermediate exchange in regular format. Average of the K_D values for the amino acids in slow exchange are in the *last line*. *C*, alignment of the three SUMO isoforms with the location of secondary structure elements, which include four β-strands and one α-helix. Amino acids involved in interaction with peptides are shown in *pink*. β_1 is shown in *purple*, β_2 in *blue*, β_3 in *yellow*, βv_4 in *red*, and the α-helix in *green*. Secondary structure elements of SUMO1 are represented in the same colors as described for *C*. *D*, binding surface analysis of SUMO1 with the $SIM_{PIASxα}$ peptide (*left*), of SUMO2 with the $SIM_{PIASxα}$ peptide (*middle*), and of SUMO2 for SIM_{TTRAP} peptide (*right*). Amino acids in slow exchange at saturation are in *fuschia*, and amino acids in intermediate exchange are in *blue*.

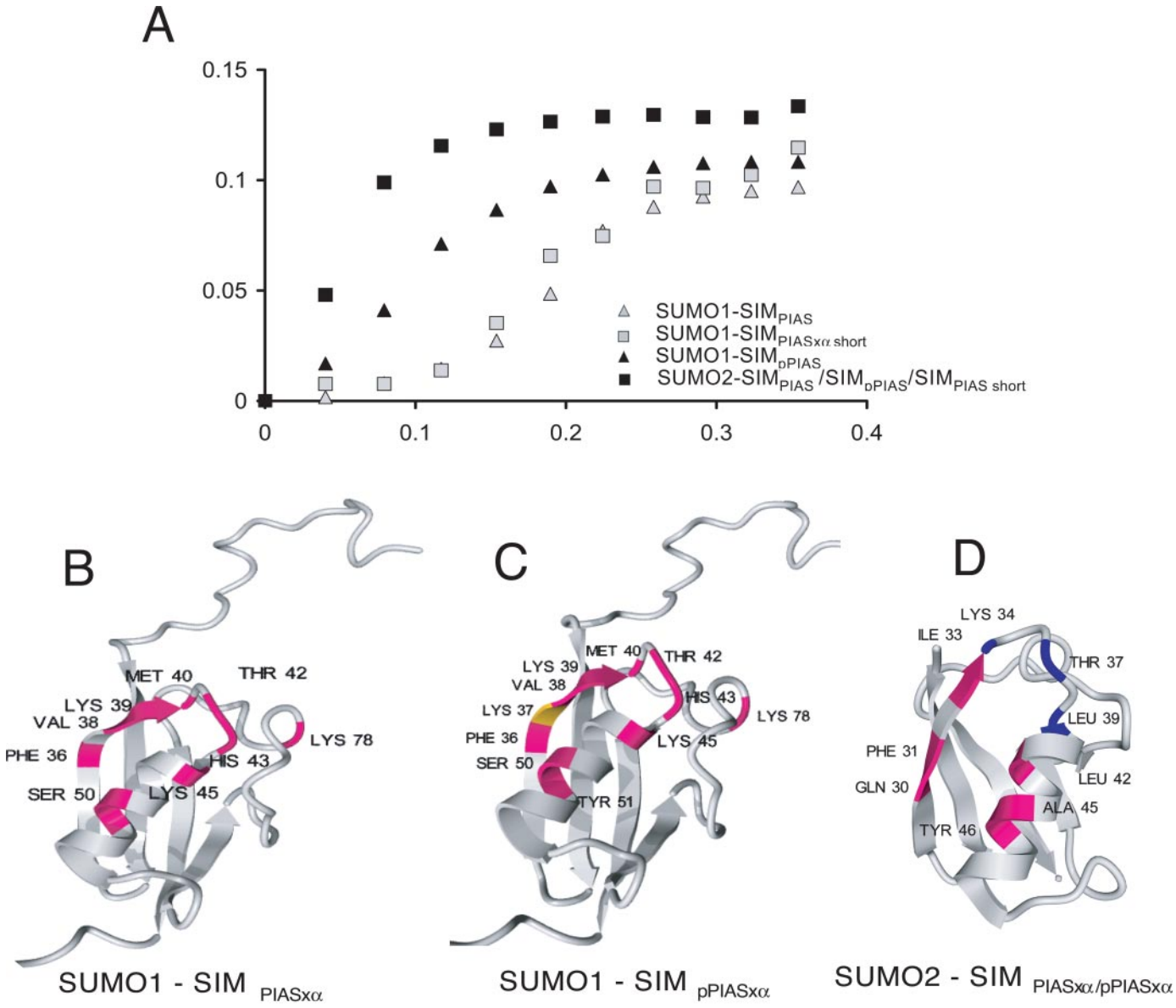

E

Sequence	Position	Phosphorylated	Unphosphorylated
KIDVIDLTIESSSDEEEDPPAKR	477-499	yes	yes
KKIDVIDLTIESSSDEEEDPPAK	476-498	yes	no
IDVIDLTIESSSDEEEDPPAKR	478-499	yes	yes
IDVIDLTIESSSDEEEDPPAK	478-498	yes	no

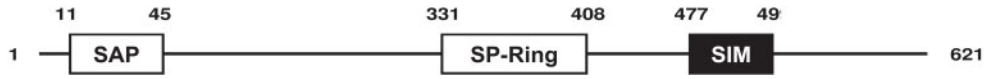

FIGURE 5. **Phosphorylation and negatively charged amino acids within the SIM alter binding to SUMO isoforms.** *A*, comparison of titration curves obtained for SUMO1 or SUMO2 with SIM$_{PIASx\alpha}$ SIM$_{pPIASx\alpha}$, or SIM$_{PIASx\alpha\ short}$. The peaks of the path are in arbitrary units resulting from normalization of ^{1}H and ^{15}N shifts. The values for SUMO1-SIM PIASx short have been multiplied by 10 for the sake of elgibility. *B*, binding surface analysis of SUMO1 for SIM$_{PIASx\alpha}$. *C*, binding surface analysis of SUMO1 for phosphorylated SIM$_{PIASx\alpha}$; Lys 37 is shown in *yellow*. *D*, binding surface analysis of SUMO2 for SIM$_{PIASx\alpha}$. *E*, list of PIAS tryptic fragments containing the SIM and detected in a phosphorylated and/or unphosphorylated form by MALDI spectrometry. *Bottom*, schematic diagram of the domain structure of PIASxα.

mode. Three explanations can be invoked for the sigmoid shape of the titration curves of SUMO1 with SIM$_{PIASx\alpha}$. The first possibility is that these peptides could have two binding interfaces on SUMO. However, our results show no evidence for a second binding site on SUMO, and the small size of SIM$_{PIASx\alpha\ short}$ makes it unlikely that it binds SUMO through two different sites. The second possibility is that SIM$_{PIASx\alpha}$ binds in different orientations to SUMO1, which can be ruled out according to the underlying calculations. Alternatively,

those peptides have only one binding site on SUMO which conformation can be changed upon binding of the peptide (induced fit).

When SUMO1 titrations with $SIM_{PIASx\alpha}$ and $SIM_{pPIASx\alpha}$ are compared, it appears that the only amino acid that has a significantly different behavior in these two titrations is Lys^{37}, which is in fast exchange with $SIM_{PIASx\alpha}$ and in fast intermediate exchange with $SIM_{pPIASx\alpha}$. This shows that the phosphate group of $SIM_{pPIASx\alpha}$ is likely to bind to SUMO1 in the neighborhood of this lysine (the same difference is observed for the Lys^{34} of SUMO2, which is equivalent to the Lys^{37} of SUMO1, confirming this hypothesis). The Lys^{37} of SUMO1 and the Lys^{34} of SUMO2 are situated at the end of the β_2-strand, which is much more bent in SUMO1 than in SUMO2. In close proximity to the Lys^{37} of SUMO1 and the Lys^{34} of SUMO1 is another lysine residue (Lys^{39} in SUMO1 and Lys^{36} in SUMO2) that cannot be observed due to HSQC peaks overlap and whose conformation is different in both SUMO isoforms: the Lys^{39} side chain of SUMO1 points into the binding site, whereas the Lys^{36} of SUMO2 points away from the SIM-binding site. Therefore it could be possible that the negatively charged phosphate group of $SIM_{pPIASx\alpha}$ interacts with the positively charged Lys^{39} of SUMO1 causing a conformational change favorable for $SIM_{pPIASx\alpha}$ binding and strongly affecting the neighboring Lys^{37}. The absence of a phosphate group in $SIM_{PIASx\alpha}$ would make this transition more difficult to achieve. A high $SIM_{PIASx\alpha}$ concentration would be required to maintain SUMO1 in the binding-favorable conformation, producing the observed two-step titration curve. Whether phosphorylation is present or not does not influence the binding of PIAS peptides to SUMO2 much, since the conformation of Lys^{34} is already favorable. The recently published structures of SUMO1 in complex with a PIAS derived peptide (17) and with a RanBP2 derived peptide (16) confirm this hypothesis. In both structures the end of the β_2-strand of SUMO1 is less bent than in the free SUMO1 (6), and the Lys^{39} side chain of SUMO1 moved away from the SIM-binding site to accommodate the peptide.

We note that the interaction between the Lys^{37} of SUMO1 and the phosphate group of $SIM_{pPIASx\alpha}$ indicates the orientation in which the SIM binds to SUMO: to take place while having the β_2-strand of SUMO binding the hydrophobic core of the SIM, those two elements must be parallel to each other. This has been recently verified by the structure published by Song *et al.* (17).

PIASxa Is Phosphorylated within the SIM in Vivo—These biophysical findings indicate that serine phosphorylation of the SIM may be relevant for *in vivo* interactions between SUMO1 and the $SIM_{PIASx\alpha}$. Accordingly, mutations of corresponding serines to alanines in the $SIM_{PIASx\alpha}$ revealed that these serines are required for its binding to SUMO1 in yeast cells (13). We therefore investigated the phosphorylation pattern of the SIM of PIASxα in cells. MALDI fingerprinting was used to verify *in vivo* phosphorylation of PIASxα at the putative phosphorylation site within the SIM. Masses corresponding to different phosphorylated fragments upon trypsin digestion contained in the SIM were observed in several spectra, in addition to less frequently observed masses corresponding the same fragments without phosphate incorporated (Fig. 5*E*; a more detailed table is given in the supplemental Fig. 3). This shows that the PIASxα proteins are phosphorylated within the SIM *in vivo* and indicates that this modification may be of functional importance for binding of SUMO1 to SIM in PIAS proteins.

We next tested whether phosphorylation of SIM is essential for binding to SUMO isoforms in GST pulldown assays. In contrast to previously published data whereby mutations of the corresponding serines to alanines in the SIM of PM-Scl75 blocked their binding to SUMO1 in yeast cells (13), we have not observed a significant decrease upon mutation of all three serine residues to alanine within the SIM motif of PIASxα (data not shown). This could be explained by a compensatory interaction between the negatively charged amino acid tract of $SIM_{PIASx\alpha}$ and $SIM_{pPIASx\alpha}$ with Lys^{78} of SUMO1 (Figs. 5, *B* and *C*). This interaction results in the similar affinity of non-phosphorylated and phosphorylated PIAS peptides binding to SUMO1 and SUMO2 (see below). Therefore, it is possible that PIAS phosphorylation *in vivo* may modulate the spatial orientation rather then affinities of PIAS binding to its sumoylated targets.

Contribution of Acidic Amino Acids in SIMs for SUMO1 and SUMO2 Binding—A number of negatively charged amino acids (Glu, Asp) are present in the SIM of most proteins found in the yeast two-hybrid screens, which indicates that they may play a regulatory role in binding to SUMO. To investigate their role, we studied the binding of SUMO to $SIM_{PIASx\alpha\ short}$ (Fig. 4*A*), a variant of the PIASxα peptide lacking the negatively charged amino acids tract. This peptide binds to SUMO1 with much lower affinity than $SIM_{PIASx\alpha}$ (no resonance of any amino acid in the SIM-binding site is observed to be in the slow exchange regime) (Fig. 4*B*). However, the resonance of amino acids Ile^{22}, Phe^{36}, Val^{38}, Lys^{39}, Lys^{45}, and Ser^{50} are in intermediate exchange. The K_D value can be estimated to be higher than for $SIM_{PIASx\alpha}$ and $SIM_{pPIASx\alpha}$ and lower than 0.2 mM, a value obtained from titration curves of amino acids of SUMO outside the SIM-binding site. When studying the titration of SUMO1 with $SIM_{PIASx\alpha}$ and with $SIM_{pPIASx\alpha}$, the resonance of Lys^{78} (situated in the loop between the β_3- and β_4-strands) was in slow exchange, whereas it was not in the $SIM_{PIASx\alpha\ short}$ titration experiment. This further supports the notion of an interaction between the negatively charged amino acid tract of $SIM_{PIASx\alpha}$ and $SIM_{pPIASx\alpha}$ with Lys^{78} of SUMO1 (Fig. 5, *B* and *C*). This interaction results in the above described higher affinity of SUMO1 for $SIM_{PIASx\alpha}$ and $SIM_{pPIASx\alpha}$ than for $SIM_{PIASx\alpha\ short}$. In contrast, results obtained in the titration of SUMO2 with $SIM_{PIASx\alpha\ short}$ are fairly similar to those obtained in the titration of SUMO2 with $SIM_{PIASx\alpha}$ and $SIM_{pPIASx\alpha}$. Furthermore, SIM_{TTRAP}, which has no tract of negatively charged amino acids, binds better to SUMO2 than to SUMO1. Taken together, these data show that negatively charged residues in the SIM make an important contribution to binding to SUMO1 but are only little involved in SUMO2 binding.

Acidic Amino Acids Influence Binding to SUMO1 but Not to SUMO2 in Vitro and in Vivo—To examine whether the observation that acidic amino acids of SIMs influence binding to SUMO paralogues is a general phenomenon, we performed mutation studies and analyzed SUMO binding in both yeast and pulldown assays. We deleted the acidic part of several SUMO-interacting partners in a similar way as PIAS short peptide was created (Fig. 6A). These mutants were transformed into yeast or were used for GST pulldown assays. The yeast deletion mutants (Sp100, Senataxin, PIAS4, TOPORS) were transformed into yeast expressing SUMO1 and SUMO2 in parallel with the corresponding wild type SUMO-interacting partners. To compare the growth of yeast three different colonies of each retransformation were replated on a fresh agar plate with the same dropout medium. After 2 days the yeast was transferred to a filter paper, and the growth of yeast expressing SUMO1 or SUMO2 and either wild type or mutant constructs was compared (Fig. 6*B*). In all cases yeast containing SUMO1 and the acidic deletion mutants grew much slower than yeast containing SUMO2 and the deletion mutants, while yeast transformed with the wild type clones grew with equal speed in both cases. Furthermore we deleted acidic amino acids of the SIM in several SUMO-interacting partners (Sp100, PIAS1, PIAS3) and expressed them in mammalian cells. In GST pulldown assays with GST-SUMO1, GST-SUMO2, and GST-SUMO3, the results were similar to those obtained with the yeast two-hybrid system: bind-

A

SUMO interacting partners	Deletion part	Deleted amino acids
Senataxin	1020-1026	DDDDDE
PIAS3	448-452	DEED
PIAS4	476-493	EDEEEEEEEEEDEDEE
Sp100	329-333	EDSE
TOPORS	911-916	DSDSD
PIAS1	464-474	DSSSDEEEEE

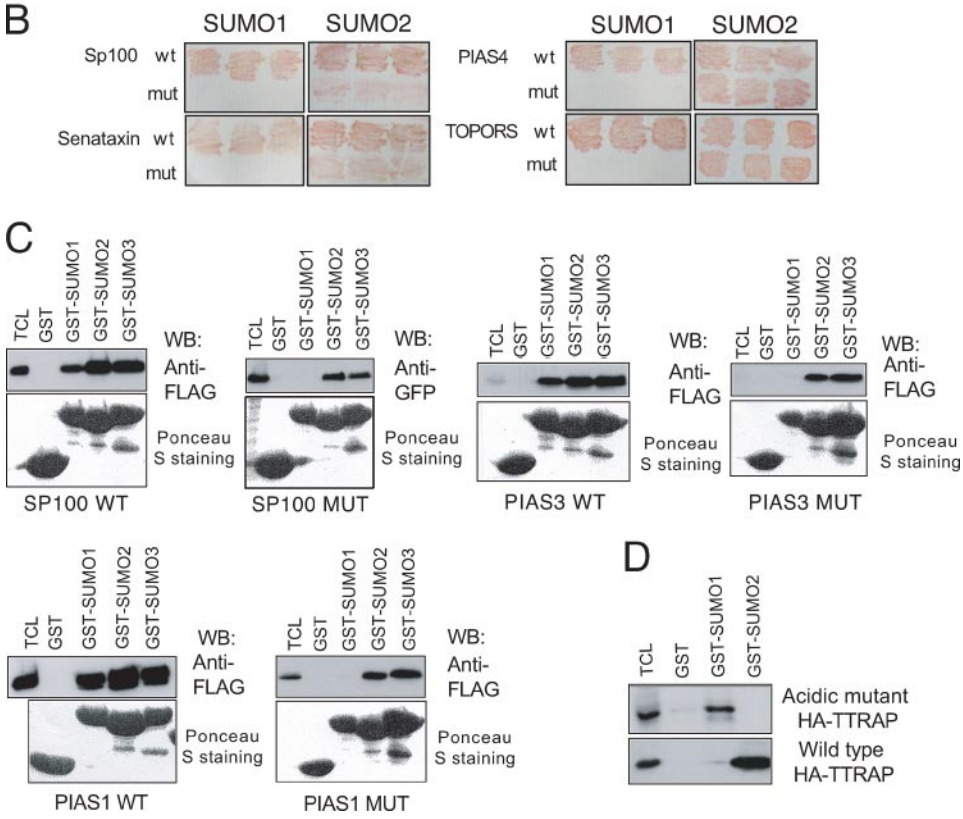

FIGURE 6. **Deletion of the acidic amino acids of the SIM influences SUMO1 much stronger than SUMO2 binding.** *A*, acidic amino acids were deleted in several SUMO-interacting partners according to the creation of the PIAS short peptide described before. The table shows the deleted part and amino acids. *B*, wild type and mutants of SUMO-interacting partners were retransformed in yeast containing SUMO1 and SUMO2 in parallel. Growth was analyzed as described before (Fig. 1*B*). *C*, lysates from HEK 293T cells expressing wild type FLAG-SP100, FLAG-PIAS1, or FLAG-PIAS3 and their corresponding mutants lacking the acidic amino acids of the SIM (EGFP-SP100 MUT, FLAG-PIAS1 MUT, or FLAG-PIAS3 MUT) were incubated with GST alone or GST-SUMO1/2/3 and analyzed by SDS-PAGE and subsequent Western blotting with indicated antibodies. Levels of GST fusion proteins were determined by Ponceau S staining. *TCL*, total cell lysate. *D*, GST pulldown of HA-TTRAP wild type and HA-TTRAP mutant containing additional acidic amino acids. The mutant with acidic amino acids binds stronger to SUMO1 but not to SUMO2, which is opposite from the wild type protein.

ing to GST-SUMO1 was reduced or even abolished, whereas binding to SUMO2/3 was unaltered (Fig. 6*C*). Taken together, these results show that acidic amino acids and negative charges are important for binding to SUMO1 but not to SUMO2/3.

The SIM of TTRAP does not contain a negative amino acid tract (Fig. 3*C*) and was shown to preferentially bind to SUMO2 compared with SUMO1 both *in vitro* and *in vivo* (Figs. 1*B*, 2*A*, and 4*B*). We were further interested in analyzing whether addition of acidic charged amino acids in TTRAP would switch its binding preference toward SUMO1 in the context of full protein. The amino acids Leu^{286}, Gly^{287}, and Lys^{288} were mutated to the negatively charged acidic amino acids Glu, Asp, and Glu, respectively. In GST pulldown assays of TTRAP wild type and TTRAP mutant, we found that the negatively charged SIM of the TTRAP mutant gains ability to bind to SUMO1, whereas the binding to SUMO2 decreased compared with the binding between TTRAP wild type and SUMO2 (Fig. 6*D*). Thus, in this case introduction of negatively charged amino acids shifts the interaction from preferential SUMO2 to SUMO1 binding.

DISCUSSION

Protein modifications mediated by conjugation of SUMO to target proteins represent an emerging mechanism by which cells control distinct cellular functions (35). While our understanding of the mechanisms of protein conjugation by SUMO are quite advanced (4, 16, 33, 36), much remains to be understood on how these modifications are translated into different biological responses. It has already been described that SIMs bind to SUMO1 via their hydrophobic core. In this report we describe molecular and biophysical parameters underlying the interactions between SUMO1 and SUMO2 and SIMs in more detail.

Several recent publications nicely describe the binding of the hydrophobic core to be the main mediator of SUMO binding. Our mutation studies in TTRAP support these results indicating that few hydrophobic amino acids are sufficient to mediate binding to SUMO. However, our *in vivo* studies in yeast show a completely different picture: only 1 out of 20 different yeast clones exclusively contains the hydrophobic core. All the others additionally contain acidic amino acids and sometimes putative phosphorylation sites. This suggests that amino acids surrounding the hydrophobic core also influence binding to SUMO.

Three different SUMO isoforms are expressed in eukaryotes, which differ mostly in the amino acid composition of the β_2-strand and the α-helix (7), exactly the regions that we found to mediate binding to SIMs. This surface of SUMO can thus be regarded as a "code of specificity" of SUMO isoforms for the SUMO-SIM interaction. Interestingly, this region has been shown to be critical for the transcriptional inhibitory properties of SUMO (37). As the signature of the SIM motif is limited to the short β-strand forming motif, it should be possible to find the intermolecular strand either in parallel or antiparallel orientation, as long as backbone hydrogen binding can occur and the hydrophobic side chains are arranged in an inverse (reverse) manner. Indeed, we and others (16, 17) found the PIASxα peptides bound parallel to the

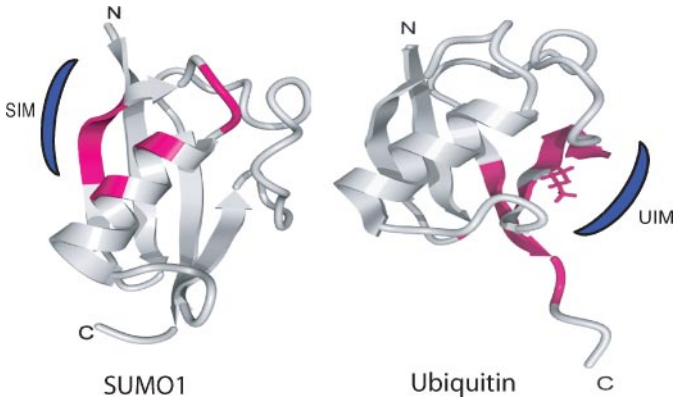

FIGURE 7. **Comparison of the SIM-binding site on SUMO1 (*left*) and the UIM-binding site on the Ub (*right*).** The SIM (*blue bow*) binds to an area defined by the second β-strand and the α-helix of SUMO, whereas the UIM (*blue bow*) binds to a group of amino acids of the third and fourth β-strands of Ub. The structures used in the figure are SUMO1 (Protein Data Bank accession code 1A5R) and UIM-Ub structure (Protein Data Bank accession code 1Q0W (41).

β_2-strand, whereas the RanBP2 fragment was shown to bind antiparallel to SUMO. Since the hydrophobic core of the SIM is preceded by acidic residues in RanBP2 and followed by acidic residues in PIAS, it can be expected that the position of the acidic residues tract observed in SIMs determine their orientation relatively to the β_2-strand of SUMO. The negative charge borne by the acidic residues tract can be furthermore supported by phosphorylation of serine residues within the SIM. Phosphorylation, as well as negatively charged acidic residues, help to maintain specificity and orientation of binding of SUMO1 to different ligands thereby increasing the affinity by providing additional electrostatic interactions.

In contrast to SUMO1 the affinity of SUMO2 does not depend on the presence of an acidic track or phosphorylation and is mainly defined by its core SIM signature. However, also SUMO2 binding does not seem to be exclusively mediated by the hydrophobic core. Both RanBP2 and the TTRAP mutant containing additional acidic amino acids do not bind to SUMO2 indicating that also in the case of SUMO2 the hydrophobic core of the SIM is not exclusively responsible for mediating binding. It remains to be investigated which residues surrounding the hydrophobic core are crucial for SUMO2 binding.

The presented concept of surrounding charges determining the orientation of a peptide binding to SUMO resembles the binding mode of polyproline stretches when interacting with SH3 domains. The polyproline type II helices bind to SH3 domains in both N-C and C-N directions while forming similar hydrogen bond networks. In analogy to the basic amino acid tract flanking P*XXP* motifs, a negatively charged tract assists binding in the case of SIM motifs. The salt bridge formed between a positively charged residue in the flanking region of the polyproline type II helix to a negative residue in the SH3 domain resembles the strong binding between Lys^{78} of SUMO1 and the negatively charged residues following the hydrophobic core of the SIM of PIASxα. The similarity found in the binding of polyproline stretches and SH3 to the SIM-SUMO interaction entails us to define SIM ligands binding in antiparallel orientation to the β_2-strand of SUMO as class I ligands (RanBP2) and those binding in parallel orientation as class II ligands (PIASxα).

Although the structures of SUMO and Ub are very similar, the binding surfaces of SUMO-SIM *versus* Ub-binding domains (UBDs) are clearly different (Fig. 7). At present, all currently tested SIMs show exclusive binding to SUMO isoforms but not to Ub or other Ub-like molecules. Although two other Ub-like proteins (NEDD8 and FAT10) have been implicated to bind to UBDs (38, 39), no known Ub-binding domain was shown to associate with SUMO isoforms, thus implicating that SUMO-SIM recognition is much more specific than Ub/NEDD8/FAT10 association with UBDs. In contrast to the formation of an intermolecular SIM-SUMO β-sheet, the interaction between UBDs and Ub is defined by a hydrophobic surface containing Ile 44 (40). This hydrophobic surface would correspond to the β_3-strand of SUMO, which is located to the opposite side of the molecule in relation to the β_2-strand where the SIM binds (Fig. 6). In principle all amino acids in the close vicinity of Ile^{44}, which are exposed to the surface, can serve as key elements defining the specificity of UBDs. Despite these structural differences, the SUMO-SIM and the Ub-UBD interactions serve the same purpose: they are signaling pairs that transmit intracellular signals and regulate numerous cell functions.

In conclusion, this study describes the molecular details of specific interactions between SUMO1 and SUMO2 paralogues and SIMs and indicates the rational for their functional differences *in vivo*.

Acknowledgments—We thank Frauke Melchior, Helene Boeuf, Jorma Palvimo, and Hans Will for help with reagents. We are also grateful to Frauke Melchior for critical comments on the manuscript and to members of the Bayer and Dikic laboratories for supporting our work and commenting on the manuscript and Ingrid Konrad for technical assistance.

REFERENCES

1. Johnson, E. S. (2004) *Annu. Rev. Biochem.* **73,** 355–382
2. Melchior, F. (2000) *Annu. Rev. Cell Dev. Biol.* **16,** 591–626
3. Ulrich, H. D. (2005) *Curr. Biol.* **15,** R257–R259
4. Hershko, A., and Ciechanover, A. (1998) *Annu. Rev. Biochem.* **67,** 425–479
5. Hay, R. T. (2005) *Mol. Cell* **18,** 1–12
6. Bayer, P., Arndt, A., Metzger, S., Mahajan, R., Melchior, F., Jaenicke, R., and Becker, J. (1998) *J. Mol. Biol.* **280,** 275–286
7. Huang, W. C., Ko, T. P., Li, S. S., and Wang, A. H. (2004) *Eur. J. Biochem.* **271,** 4114–4122
8. Sternsdorf, T., Puccetti, E., Jensen, K., Hoelzer, D., Will, H., Ottmann, O. G., and Ruthardt, M. (1999) *Mol. Cell. Biol.* **19,** 5170–5178
9. Kamitani, T., Nguyen, H. P., Kito, K., Fukuda-Kamitani, T., and Yeh, E. T. (1998) *J. Biol. Chem.* **273,** 3117–3120
10. Saitoh, H., and Hinchey, J. (2000) *J. Biol. Chem.* **275,** 6252–6258
11. Azuma, Y., Arnaoutov, A., and Dasso, M. (2003) *J. Cell Biol.* **163,** 477–487
12. Ayaydin, F., and Dasso, M. (2004) *Mol. Biol. Cell* **15,** 5208–5218
13. Minty, A., Dumont, X., Kaghad, M., and Caput, D. (2000) *J. Biol. Chem.* **275,** 36316–36323
14. Song, J., Durrin, L. K., Wilkinson, T. A., Krontiris, T. G., and Chen, Y. (2004) *Proc. Natl. Acad. Sci. U. S. A.* **101,** 14373–14378
15. Hannich, J. T., Lewis, A., Kroetz, M. B., Li, S. J., Heide, H., Emili, A., and Hochstrasser, M. (2005) *J. Biol. Chem.* **280,** 4102–4110
16. Reverter, D., and Lima, C. D. (2005) *Nature* **435,** 687–692
17. Song, J., Zhang, Z., Hu, W., and Chen, Y. (2005) *J. Biol. Chem.* **280,** 40122–40129
18. Pype, S., Declercq, W., Ibrahimi, A., Michiels, C., Van Rietschoten, J. G., Dewulf, N., de Boer, M., Vandenabeele, P., Huylebroeck, D., and Remacle, J. E. (2000) *J. Biol. Chem.* **275,** 18586–18593
19. Haglund, K., Ivankovic-Dikic, I., Shimokawa, N., Kruh, G. D., and Dikic, I. (2004) *J. Cell Sci.* **117,** 2557–2568
20. Ayed, A., Mulder, F. A., Yi, G. S., Lu, Y., Kay, L. E., and Arrowsmith, C. H. (2001) *Nat. Struct. Biol.* **8,** 756–760
21. Bairoch, A., and Apweiler, R. (1997) *Nucleic Acids Res.* **25,** 31–36
22. Benton, D. (1990) *Nucleic Acids Res.* **18,** 1517–1520
23. Bucher, P., Karplus, K., Moeri, N., and Hofmann, K. (1996) *Comput. Chem.* **20,** 3–23
24. Henikoff, S., and Henikoff, J. G. (1992) *Proc. Natl. Acad. Sci. U. S. A.* **89,** 10915–10919
25. Hofmann, K. (2000) *Brief Bioinform.* **1,** 167–178
26. Weger, S., Hammer, E., and Engstler, M. (2003) *Exp. Cell Res.* **290,** 13–27
27. Kunapuli, P., Somerville, R., Still, I. H., and Cowell, J. K. (2003) *Oncogene* **22,** 3417–3423
28. Shou, Z., Yamada, K., Kawata, H., Yokoyama, O., and Miyamoto, K. (2004) *Biochem. Biophys. Res. Commun.* **314,** 885–890
29. Moreira, M. C., Klur, S., Watanabe, M., Nemeth, A. H., Le Ber, I., Moniz, J. C., Tranchant, C., Aubourg, P., Tazir, M., Schols, L., Pandolfo, M., Schulz, J. B., Pouget, J., Calvas, P., Shizuka-Ikeda, M., Shoji, M., Tanaka, M., Izatt, L., Shaw, C. E., M'Zahem, A., Dunne, E., Bomont, P., Benhassine, T., Bouslam, N., Stevanin, G., Brice, A., Guimaraes, J., Mendonca, P., Barbot, C., Coutinho, P., Sequeiros, J., Durr, A., Warter, J. M.,

and Koenig, M. (2004) *Nat. Genet.* **36,** 225–227
30. Eladad, S., Ye, T. Z., Hu, P., Leversha, M., Beresten, S., Matunis, M. J., and Ellis, N. A. (2005) *Hum. Mol. Genet* **14,** 1351–1365
31. Kawabe, Y., Seki, M., Seki, T., Wang, W. S., Imamura, O., Furuichi, Y., Saitoh, H., and Enomoto, T. (2000) *J. Biol. Chem.* **275,** 20963–20966
32. Muller, S., Ledl, A., and Schmidt, D. (2004) *Oncogene* **23,** 1998–2008
33. Tatham, M. H., Kim, S., Jaffray, E., Song, J., Chen, Y., and Hay, R. T. (2005) *Nat. Struct. Mol. Biol.* **12,** 67–74
34. Macauley, M. S., Errington, W. J., Okon, M., Scharpf, M., Mackereth, C. D., Schulman, B. A., and McIntosh, L. P. (2004) *J. Biol. Chem.* **279,** 49131–49137
35. Haglund, K., and Dikic, I. (2005) *EMBO J.* **24,** 1–7
36. Pichler, A., Knipscheer, P., Saitoh, H., Sixma, T. K., and Melchior, F. (2004) *Nat. Struct. Mol. Biol.* **11,** 984–991
37. Chupreta, S., Holmstrom, S., Subramanian, L., and Iniguez-Lluhi, J. A. (2005) *Mol. Cell. Biol.* **25,** 4272–4282
38. Hipp, M. S., Raasi, S., Groettrup, M., and Schmidtke, G. (2004) *J. Biol. Chem.* **279,** 16503–16510
39. Tanaka, T., Kawashima, H., Yeh, E. T., and Kamitani, T. (2003) *J. Biol. Chem.* **278,** 32905–32913
40. Hicke, L., Schubert, H. L., and Hill, C. P. (2005) *Nat. Rev. Mol. Cell. Biol.* **6,** 610–621
41. Swanson, K. A., Kang, R. S., Stamenova, S. D., Hicke, L., and Radhakrishnan, I. (2003) *EMBO J.* **22,** 4597–4606
42. Delaglio, F., Grzesiek, S., Vuister, G. W., Zhu, G., Pfeifer, J., and Bax, A. (1995) *J. Biomol. NMR* **6,** 277–293